

# Learning Association via Track–Detection Matching for Multi-Object Tracking

Momir Adžemović 

Department of Computer Science, Faculty of Mathematics,  
University of Belgrade, Studentski trg 16, 11000 Belgrade, Serbia  
pd222011@alas.matf.bg.ac.rs

**Abstract.** Multi-object tracking aims to maintain object identities over time by associating detections across video frames. Two dominant paradigms exist in literature: tracking-by-detection methods, which are computationally efficient but rely on handcrafted association heuristics, and end-to-end approaches, which learn association from data at the cost of higher computational complexity. We propose Track–Detection Link Prediction (TDLP), a tracking-by-detection method that performs per-frame association via link prediction between tracks and detections, i.e., by predicting the correct continuation of each track at every frame. TDLP is architecturally designed primarily for geometric features such as bounding boxes, while optionally incorporating additional cues, including pose and appearance. Unlike heuristic-based methods, TDLP learns association directly from data without handcrafted rules, while remaining modular and computationally efficient compared to end-to-end trackers. Extensive experiments on multiple benchmarks demonstrate that TDLP consistently surpasses state-of-the-art performance across both tracking-by-detection and end-to-end methods. Finally, we provide a detailed analysis comparing link prediction with metric learning–based association and show that link prediction is more effective, particularly when handling heterogeneous features such as detection bounding boxes. Our code is available at <https://github.com/Robotmurlock/TDLP>.

**Keywords:** deep learning · multi-object tracking · tracking-by-detection · link prediction

## 1 Introduction

Multi-object tracking (MOT) aims to localize and maintain the identities of multiple objects over time and is a core component of many video-based perception systems. It is important in a wide range of applications, including autonomous driving [9,14], sports analytics [16,15], retail analytics [23], robotics [43], and surveillance [40]. Despite significant advances in object detection, MOT remains challenging: occlusions, crowded scenes, camera motion, and highly dynamic, non-linear trajectories place strong demands on both accuracy and efficiency.

Most modern MOT approaches adopt the tracking-by-detection paradigm, in which object detections are obtained independently for each frame and subsequently associated across time [47,4,11,44,1]. Early methods such as SORT [6]

and DeepSORT [41] formalized this as a per-frame bipartite matching problem between existing tracks and current frame detections. These approaches usually rely on Kalman filtering for motion prediction and optionally use appearance features [47,4,44,11,29,38,25,24]. Their performance further depends on carefully designed heuristics. While such trackers are computationally efficient, their reliance on domain-specific assumptions limits their ability to generalize across datasets. At the other end of the spectrum, fully end-to-end MOT methods learn detection and association jointly from data [46,19,20,1] and therefore require no handcrafted association rules. However, they usually require large training datasets and high computational cost. As a result, they are often too slow for real-time use [46,19,20]. This creates a gap between efficient heuristic-based trackers and expressive but computationally expensive end-to-end methods.

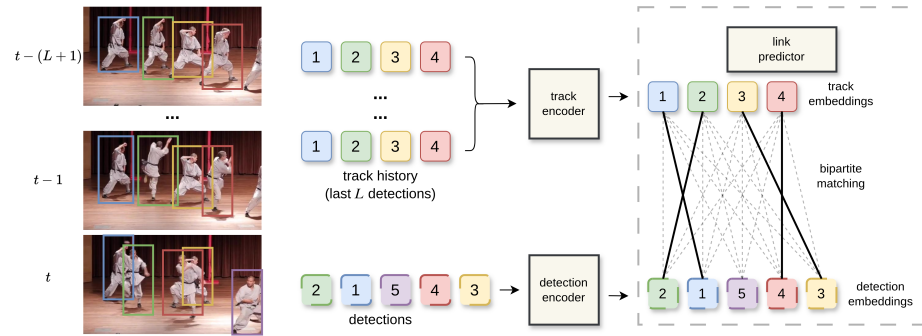


**Fig. 1.** High-level overview of the proposed association pipeline. Encoded track histories and current detections are linked via link prediction and associated using bipartite matching.

In this work, we propose Track–Detection Link Prediction (TDLP), a tracking-by-detection method that lies between heuristic-based association and fully end-to-end learning. TDLP formulates data association as a per-frame link prediction problem between existing tracks and current frame detections. Track and detection features are first embedded into compact vector representations, and link probabilities are then predicted between these vectors. A high-level overview is shown in Figure 1. TDLP learns association directly from data without handcrafted rules and maintains lower computational cost than end-to-end methods during both training and inference. To improve tracking accuracy, the method employs an architecture designed to model non-linear patterns in real-world data. It further supports feature aggregation from multiple modalities, including bounding boxes, appearance, and human pose keypoints. Even without appearance features, TDLP outperforms heuristic-based methods on datasets characterized by non-linear motion. When additional cues are incorporated,

TDLP achieves state-of-the-art performance on DanceTrack [39], SportsMOT [16], SoccerNet [15], and BEE24 [12]. The contributions of this paper are as follows:

- We propose TDLP, a learning-based association method that performs per-frame bipartite matching via link prediction, leveraging advanced motion modeling and multi-modal feature aggregation.
- We design a SORT-like tracking framework based on TDLP that surpasses the state of the art. Notably, when using only detector-provided bounding boxes, our method outperforms all heuristic-based trackers, including those that use object appearance cues.
- We analyze the proposed link-prediction formulation and compare it with alternative association methods such as metric learning, identifying the key factors that cause metric learning to underperform relative to our approach.

## 2 Related Work

**Heuristic-based tracking-by-detection.** Modern tracking-by-detection methods largely build on the two-stage association strategy introduced by ByteTrack [47], which first associates high-confidence detections before considering low-confidence ones. Subsequent works extend this pipeline with engineered heuristics, such as exploiting perspective effects via object height or image-plane position [3,44,25,38], incorporating detection confidence [38,44,2], compensating for camera motion [4,29,44,45], or using improved motion models [22,42,3,2,11]. While effective, such heuristics are often dataset- and scenario-dependent and require careful hyper-parameter tuning. In literature, they tend to perform better on crowded datasets with relatively linear motion, such as MOTChallenge [17], than on datasets with non-linear motion and visually similar objects, such as DanceTrack [39] and SportsMOT [16,1]. In contrast, our approach removes hand-crafted association rules and learns the association function directly from data. This enables adaptive weighting of cues based on their reliability and improves robustness on datasets with non-linear motion.

**End-to-end tracking.** End-to-end trackers jointly perform detection and association within a single model, avoiding explicit heuristics. Since MOTR [46], this line of work has steadily advanced and achieves strong performance on challenging benchmarks such as DanceTrack [19,20,39]. However, end-to-end methods are computationally expensive to train and deploy [46,20,10], and their tightly coupled design reduces modularity and complicates component-level modifications. Our method offers a simpler alternative that retains the benefits of learned association while preserving the efficiency and modularity of tracking-by-detection pipelines. By optionally incorporating appearance features, it enables a direct trade-off between accuracy and inference speed.

**Offline graph-based methods.** Our work is related to offline graph-based trackers such as MPNTrack [8] and SUSHI [13], which formulate data association as a link prediction problem over spatio-temporal graphs. These methods perform global optimization over video clips and exploit long-range temporal context.

However, they operate offline and require access to future frames, limiting their applicability in real-time scenarios. In contrast, our architectural design performs link prediction online by modeling associations between tracks and detections as track continuations.

**Tracking-by-detection with learned association.** Concurrent works propose using metric learning to learn associations between tracks and detections, where embeddings are matched using distance metrics such as cosine or normalized Euclidean distance [36,31]. However, metric learning enforces a global embedding structure, which can be restrictive when handling heterogeneous features, particularly low-dimensional geometric cues such as bounding boxes. In such settings, embeddings may remain close unless differences accumulate across multiple feature dimensions, leading to incorrect associations even when a mismatch in a single cue should be sufficient. In contrast, the link prediction model outputs similarity at the feature level and can emphasize the most informative differences between objects, making it particularly suitable for geometric association. We analyze this distinction in Section 4.2 and show that link prediction consistently outperforms contrastive learning when using bounding-box features.

### 3 Methodology

We formulate per-frame association as a bipartite link prediction problem between tracks and detections, define the corresponding optimization objective, and present the TDLP architecture and tracking pipeline used for frame-wise association.

#### 3.1 Track–detection bipartite link prediction

We consider an online MOT setting where, at each frame  $t$ , we maintain a set of active tracks  $\mathcal{T}_t = \{T_1, \dots, T_{N_t}\}$  and a set of detections  $\mathcal{D}_t = \{D_1, \dots, D_{M_t}\}$  produced by an object detector. Each track  $T_i$  is represented by a short temporal window of length  $L$  containing its most recent observations. Our objective is to estimate the association matrix  $\mathbf{Y}_t \in \{0, 1\}^{N_t \times M_t}$ , where  $Y_{ij} = 1$  if detection  $D_j$  is the correct continuation of track  $T_i$  at frame  $t$ , and  $Y_{ij} = 0$  otherwise. In other words, we aim to approximate the adjacency matrix of the bipartite graph formed between tracks and detections.

Our proposed link prediction pipeline proceeds as follows. Let  $f_t$  and  $f_d$  denote the track and detection encoder functions, respectively. These functions transform the raw input features into a unified embedding space. For each track  $T_i$  and detection  $D_j$ , the model computes

$$\mathbf{e}_i^{\text{trk}} = f_t(T_i), \quad \mathbf{e}_j^{\text{det}} = f_d(D_j). \quad (1)$$

Here,  $\mathbf{e}_i^{\text{trk}}$  and  $\mathbf{e}_j^{\text{det}}$  are the encoded representations produced by the architecture described in Section 3.2. The link probability for each pair  $(i, j)$  is then predicted as

$$S_{ij} = \phi(\mathbf{e}_i^{\text{trk}}, \mathbf{e}_j^{\text{det}}), \quad (2)$$

where  $\phi$  denotes the track–detection link prediction function. The resulting score  $S_{ij} \in (0, 1)$  is interpreted as the probability that track  $T_i$  and detection  $D_j$  correspond to the same trajectory and should therefore be linked.

In order to find  $f_t$ ,  $f_d$  and  $\phi$ , we sample video clips from the dataset and optimize the weighted binary cross-entropy (BCE) loss between all positive and negative track–detection pairs:

$$\mathcal{L}_{\text{BCE}} = - \sum_{i=1}^{N_t} \sum_{j=1}^{M_t} \left( w^+ Y_{ij} \log S_{ij} + (1 - Y_{ij}) \log(1 - S_{ij}) \right), \quad (3)$$

where  $Y_{ij}$  is derived from ground-truth identities. The parameter  $w^+ > 1$  controls the positive-class weighting and compensates for the strong imbalance between positive and negative samples, i.e., the fact that most track–detection pairs correspond to negative links. Only the final clip frame contributes to the supervision.

At inference time, the scores  $S_{ij}$  define the edge weights in a bipartite matching between tracks and detections, and a simple linear assignment (e.g. Hungarian algorithm) [34] is applied to obtain the predicted associations.

### 3.2 Architecture

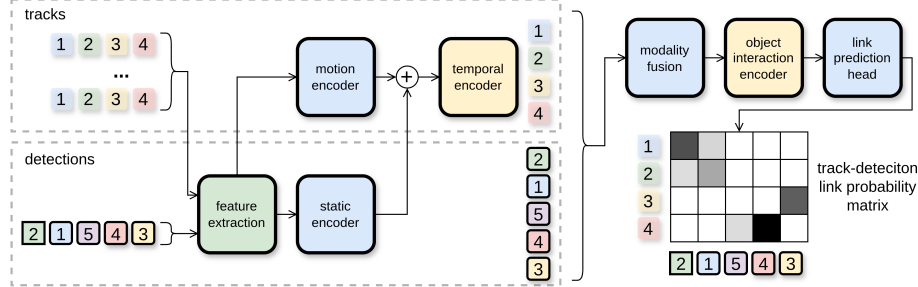


**Fig. 2.** Architecture overview of the proposed TDLP method. Tracks and detections first undergo a geometric feature transformation, while optional additional cues (e.g., pose keypoints and appearance) are extracted using dedicated models. The static encoder processes per-frame detections from both current detections and track histories, while a motion encoder extracts track-specific temporal features (e.g., velocity). Track features are aggregated over time using a temporal encoder transformer. The resulting track and detection embeddings are fused across modalities and refined by an object-interaction encoder transformer. Finally, a link prediction head outputs association probabilities for each track–detection pair.

The TDLP architecture (Figure 2) follows a transformer-encoder design that maps tracks and detections into representations suitable for bipartite link

prediction. The baseline variant, *TDLP-bbox*, uses only bounding box geometry and confidence scores, while additional modalities (e.g., appearance) can be incorporated to improve accuracy. The pipeline consists of three stages: (i) feature extraction, (ii) feature encoding, and (iii) link prediction.

**Feature extraction.** Prior work shows that simple geometric transformations can improve tracking accuracy [3,2,42,22]. Following this, we adopt a feature extraction pipeline tailored to link prediction. At time  $t$ , the model processes up to  $N_t \cdot L + M_t$  detections, where  $N_t$  is the number of active tracks,  $L$  the history length, and  $M_t$  the number of current detections. Let  $x_{i,t}$  denote the detection features of object  $i$  at time  $t$ .

To reduce sensitivity to absolute image coordinates and improve generalization across clips, we apply *frame-wise min–max normalization* to all geometric features, mapping each coordinate to  $[0, 1]$ :

$$\tilde{x} = \frac{x - x_{\min}}{x_{\max} - x_{\min}}. \quad (4)$$

To capture rough motion patterns, we compute *first-order differences* for each track:

$$\Delta x_{i,t} = \frac{x_{i,t} - x_{i,\tau}}{t - \tau}, \quad (5)$$

where  $\tau$  denotes the time index of the most recent observation of object  $i$ . This operation is applied only to tracks, as detections lack a temporal dimension and therefore do not support temporal differences. Finally, all feature dimensions are *standardized* to zero mean and unit variance. These transformations are general and domain-agnostic, and naturally extend to additional geometric modalities such as human pose keypoints (hereafter referred to as *keypoints*).

Track and detection features cannot be processed by a shared encoder because their feature sets may differ (e.g., velocity estimates are defined only for tracks). Accordingly, we use a static encoder  $f_{\text{stat}}$  for all point observations and a motion encoder  $f_{\text{mot}}$  for track-specific features. The resulting input embeddings are

$$\mathbf{h}_{i,t-k} = f_{\text{stat}}(x_{i,t-k}) + f_{\text{mot}}(\Delta x_{i,t-k}), \quad \mathbf{h}_{j,t} = f_{\text{stat}}(x_{j,t}), \quad (6)$$

where  $k \in \{1, 2, \dots, L\}$ .

Appearance features extracted from re-identification (ReID) models are commonly used to improve association performance [4,24,29,2,44]. Thus, our architecture supports the inclusion of additional modalities that can be derived from detections (e.g., appearance, keypoints, or other object attributes). In the remainder of the text, we use  $x_{i,t}^{(m)}$  to denote a  $C$ -dimensional feature vector of modality  $m$  for the  $i$ -th object at time  $t$ .

**Temporal transformer encoder.** For temporal track modeling, we adopt the motion encoder from TransFilter [2], a transformer architecture that is robust to trajectory truncation via reversed positional encoding (RPE). Since our objective is to obtain a track embedding for the next frame rather than predict a bounding box, we remove the prediction head and use the transformer output directly:

$$\mathbf{z}_i^{trk} = f_{\text{temporal}}(\mathbf{h}_{i,t-L:t-1}), \quad (7)$$

where  $f_{\text{temporal}}$  denotes the temporal transformer encoder and  $\mathbf{h}_{i,t-L:t-1}$  is the sequence of input embeddings for track  $i$ . For detections,  $z_j^{\text{det}} = h_{j,t}$ .

**Multi-modal fusion.** After track temporal encoding, each object yields modality-specific tokens  $\mathbf{z}^{(m)}_{m \in \mathcal{M}}$ . Inspired by CAMELTrack [36], we map each modality into a shared embedding space via a learned linear projection  $\mathbf{W}^{(m)}$ , and the final multi-modal token is obtained by summing the projected embeddings:

$$\mathbf{u} = \sum_{m \in \mathcal{M}} \mathbf{W}^{(m)} \mathbf{z}^{(m)}. \quad (8)$$

**Object interaction encoder.** To model interactions between objects within the same frame, we apply transformer-style encoders to both tracks and detections. A single-modality interaction encoder is first applied independently to each modality (omitted in Figure 2 to avoid clutter). After multi-modal fusion, a joint interaction encoder processes all tokens:

$$\{\bar{\mathbf{z}}_i^{\text{trk}}\}_i, \{\bar{\mathbf{z}}_j^{\text{det}}\}_j = f_{\text{inter}}(\{\mathbf{u}_i^{\text{trk}}\}_i \cup \{\mathbf{u}_j^{\text{det}}\}_j), \quad (9)$$

where  $f_{\text{inter}}$  is a transformer encoder applied over the combined set of multi-modal track and detection tokens. This stage allows tracks and detections to attend to each other and refine their representations before link prediction.

**Bipartite link prediction head.** Given refined track and detection embeddings  $\bar{\mathbf{z}}_i^{\text{trk}}$  and  $\bar{\mathbf{z}}_j^{\text{det}}$ , TDLP performs link prediction on the track–detection bipartite graph. For each pair  $(i, j)$ , we construct a pairwise representation

$$\mathbf{v}_{ij} = [\bar{\mathbf{z}}_i^{\text{trk}}, \bar{\mathbf{z}}_j^{\text{det}}, |\bar{\mathbf{z}}_i^{\text{trk}} - \bar{\mathbf{z}}_j^{\text{det}}|], \quad (10)$$

where  $[\cdot]$  denotes concatenation and  $|\cdot|$  the element-wise absolute value. A shallow MLP  $\phi$  outputs the link probability  $S_{ij}$  used in Eq. (3). At inference, the resulting scores define the cost matrix for linear assignment.

### 3.3 The tracker

For tracking inference, TDLP follows the same high-level workflow as SORT [6] (or DeepSORT [41] when appearance features are used), but without any hand-crafted association heuristics. For each frame, detections are first obtained and filtered using the detection threshold  $\theta_{\text{det}}$  to remove low-confidence observations. The remaining detections are optionally enriched with additional features, and TDLP computes probabilistic link scores for every track–detection pair. During association, candidate links are considered only if their predicted probability exceeds the gating threshold  $\theta_{\text{link}}$ , after which the final one-to-one matching is computed using the Hungarian algorithm [34].

After association, the track life cycle is updated as follows. An unmatched detection provides evidence for initializing a new track, which becomes confirmed only after accumulating at least  $T_{\text{init}}$  successful associations and meeting the detection-confidence requirement  $\theta_{\text{new}}$ . Unmatched tracks are retained for up to  $T_{\text{lost}}$  frames and removed if no compatible detection appears within this window.

## 4 Experimental Analysis

We evaluate on five MOT datasets: DanceTrack [39], SportsMOT [16], SoccerNet [15], MOT17 [17], and BEE24 [12]. We report results for two variants: *TDLP*, which combines bounding boxes, human pose keypoints, and appearance features, and the lightweight *TDLP-bbox*, which uses only bounding box features. We primarily report HOTA, along with AssA and IDF1 to emphasize association performance [28]. All implementation details are provided in Appendix A.

### 4.1 Benchmarks

**DanceTrack.** DanceTrack<sup>1</sup> is a multi-object tracking dataset of dance videos. It is particularly challenging due to visually similar performers, frequent occlusions, and fast, non-linear motion. The dataset spans diverse styles, including classical, street, pop, large-group, and sports performances, making it a demanding benchmark [39]. In literature, the leaderboard is dominated by end-to-end trackers such as MOTIP [20] and MeMOTR [19], which typically outperform tracking-by-detection methods due to the dataset’s strong emphasis on association difficulty.

As shown in Table 1, TDLP outperforms both end-to-end and tracking-by-detection methods, improving over the previous state-of-the-art (CAMELTrack) by 0.8% HOTA and 0.9% IDF1. Interestingly, the lightweight *TDLP-bbox* variant surpasses all heuristic-based trackers despite relying only on bounding box features, without using appearance cues.

Method	HOTA	DetA	AssA	MOTA	IDF1
<i>e2e</i>					
MOTR [46]	54.2	73.5	40.2	79.7	51.5
MOTIP [20]	67.5	71.6	57.6	90.3	72.2
MeMORT [19]	68.5	71.6	58.4	89.9	71.2
<i>tbd (bbox features)</i>					
ByteTrack [47]	47.3	71.6	31.4	89.5	52.5
OC_SORT [11]	55.1	80.4	38.0	89.4	54.9
MoveSORT [3]	56.1	81.6	38.7	91.8	56.0
<b>TDLP-bbox (ours)</b>	<b>67.8</b>	<b>82.2</b>	<b>56.1</b>	<b>91.9</b>	<b>72.7</b>
<i>tbd (extra features)</i>					
Deep OC_SORT [29]	61.3	81.6	45.8	91.8	61.5
DeepMoveSORT [2]	63.0	82.0	48.6	<b>92.6</b>	65.0
Hybrid-SORT [44]	65.7	-	-	91.8	67.4
CAMELTrack [36]	69.3	81.8	58.9	91.4	74.9
<b>TDLP (ours)</b>	<b>70.1</b>	<b>82.6</b>	<b>59.6</b>	91.8	<b>75.8</b>

**Table 1:** Evaluation results on the DanceTrack test set. *e2e* denotes end-to-end methods and *tbd* tracking-by-detection. All *tbd* methods use the public YOLOX detector, while *e2e* methods employ their own detectors.

**SportsMOT.** SportsMOT<sup>2</sup> is a large-scale MOT dataset spanning basketball, volleyball, and football. It is challenging due to visually similar players and

<sup>1</sup> DanceTrack GitHub page: <https://github.com/DanceTrack/DanceTrack>.

<sup>2</sup> SportsMOT GitHub page: <https://github.com/MCG-NJU/SportsMOT>.

highly non-linear motion with frequent accelerations, decelerations, and direction changes, as well as diverse match scenarios and camera viewpoints [16]. On this benchmark, tracking-by-detection methods combining heuristics with learnable motion models perform strongly [3,2,22,42], often outperforming current end-to-end trackers.

As shown in Table 2, TDLP outperforms both end-to-end and tracking-by-detection methods on SportsMOT, establishing a new state-of-the-art. Compared to the previous best method, CAMELTrack, TDLP improves HOTA by 1.5% and IDF1 by 3.1%. The larger gains in association metrics relative to DanceTrack are expected, as SportsMOT places stronger emphasis on accurate motion modeling due to highly non-linear player trajectories. In this setting, TDLP’s stronger motion modeling yields more pronounced benefits. Notably, the lightweight *TDLP-bbox* variant outperforms all prior motion-only methods without relying on appearance features or validation-based detector tuning.

Method	Training setup	HOTA	DetA	AssA	MOTA	IDF1
<i>e2e</i>						
MeMORT [19]	Train	70.0	83.1	59.1	91.5	71.4
MOTIP [20]	Train	71.9	83.4	62.0	92.9	75.0
<i>tbd (bbox features)</i>						
ByteTrack [47]	Train	62.8	77.1	51.2	94.1	69.8
OC_SORT [11]	Train	71.9	86.4	59.8	94.5	72.2
MoveSORT [3]	Train+Val	74.6	87.5	63.7	96.7	76.9
<b>TDLP-bbox (ours)</b>	Train	74.8	87.2	64.1	95.4	79.0
<i>tbd (extra features)</i>						
Deep-EIoU [24]	Train	74.1	87.2	63.1	95.1	75.0
Deep-EIoU [24]	Train+Val	77.2	88.2	67.7	96.3	79.8
DeepMoveSORT [2]	Train+Val	78.7	88.1	70.3	<b>96.5</b>	81.7
CAMELTrack [36]	Train	80.4	<b>88.8</b>	72.8	96.3	84.8
<b>TDLP (ours)</b>	Train	<b>81.9</b>	88.0	<b>76.3</b>	95.8	<b>87.5</b>

**Table 2:** Evaluation results on the SportsMOT test set. Acronyms *e2e* and *tbd* denote end-to-end and tracking-by-detection methods. *Training setup* indicates whether the validation set was additionally used during training for the submitted solutions [16].

**BEE24.** BEE24<sup>3</sup> is a recent MOT benchmark for ecological scenarios, comprising video sequences of bees recorded under natural conditions. It is highly challenging due to crowded scenes, frequent occlusions, rapid and irregular motion, and near-identical appearances. By introducing a non-human domain with fundamentally different visual and motion characteristics, BEE24 complements existing human-focused MOT benchmarks and provides a valuable testbed for evaluating robustness and generalization.

Table 3 reports results on BEE24, where TDLP improves over the previous state-of-the-art by 1.6% HOTA and 3.0% IDF1. The gains in association accuracy are particularly notable, as BEE24 is the most challenging benchmark in terms of motion prediction, with dense interactions, occlusions, and highly irregular

<sup>3</sup> BEE24 (TOPICTrack) GitHub page: <https://github.com/holmescao/TOPICTrack>

trajectories. Unlike human-tracking datasets, we rely solely on bounding box features, since keypoints and appearance embeddings are unavailable and appearance cues are inherently limited. While orientation could be informative [7], it is not provided, further highlighting the effectiveness of TDLP’s motion modeling.

Method	HOTA	AssA	IDF1	MOTA
<i>e2e</i>				
TrackFormer [30]	44.3	42.3	53.9	41.5
<i>tbd</i> ( <i>bbox features</i> )				
ByteTrack [47]	43.2	38.3	56.8	59.2
OC-SORT [11]	42.7	36.8	55.3	61.6
TOPICTrack [12]	46.6	40.3	59.7	66.7
CAMELTrack [36]	50.3	42.6	63.8	<b>75.7</b>
<b>TDLP-bbox (ours)</b>	<b>51.9</b>	<b>46.2</b>	<b>66.8</b>	74.9

**Table 3:** Evaluation results on the BEE24 test set. All *tbd* trackers use the same object detector.

Additional benchmark results, including experiments on MOT17 [17] and SoccerNet [15], are provided in Appendix B.

## 4.2 Ablation Studies and Discussion

**Component ablation study.** We use CTDP (contrastive track–detection learning) as the baseline, which shares the TDLP architecture but replaces the link-prediction head with a contrastive objective. Following [36], we adopt the InfoNCE loss [32] and train directly on clips without batch sampling, as it provides no measurable benefit. Results are shown in Table 4. We find that both the training objective and carefully designed motion features are critical for performance, with larger gains in the bounding-box-only setting and smaller relative improvements when keypoints and appearance are included. Compared to CTDP, TDLP improves HOTA by 11.1% (bbox-only) and 5.4% (full modalities) on DanceTrack, and by 14.0% and 11.3%, respectively, on SportsMOT.

**Feature ablation study.** We analyze TDLP variants using a single feature modality (Table 5). Combining all modalities yields the best performance. When used in isolation, bounding boxes and keypoints perform strongly, while appearance features alone are markedly weaker. This contrasts with [36], where appearance cues are more effective, whereas our motion-based features contribute more substantially. We attribute the weaker appearance-only results to a mismatch between metric-learning–based appearance pretraining and the link-prediction training objective.

**Analysis of link prediction compared to contrastive prediction.** We conduct additional experiments to understand why link prediction outperforms contrastive prediction under a fixed architecture. We focus on the bounding-box-only setting using  $(x, y, w, h, c)$ , as these low-dimensional geometric features provide a controlled environment for isolating the learning objective. Starting from a single feature  $(x)$ , we progressively add  $y, w, h$ , and  $c$ . As shown in Figure 3,

Components		DanceTrack		SportsMOT	
GFT	Method	Bb	MM	Bb	MM
Yes	TDLP	<b>62.1</b>	<b>65.4</b>	<b>80.4</b>	<b>88.4</b>
Yes	CTDP	56.7	62.3	71.8	76.8
No	CTDP	51.0	60.1	66.4	77.1

**Table 4:** Ablation of *geometric feature transform* (GFT) and link prediction (TDLP).

Features		DanceTrack		SportsMOT		
App	Kp	Bb	HOTA	IDF1	HOTA	IDF1
✓	✓	✓	<b>65.3</b>	<b>70.5</b>	<b>88.8</b>	<b>92.9</b>
✓			40.2	42.6	74.1	76.0
		✓	58.4	62.2	80.7	84.7
			✓	61.6	66.2	80.4
						83.9

**Table 5:** Feature-type ablation results for TDLP on DanceTrack and SportsMOT.

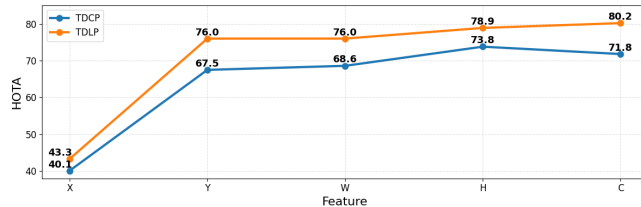


**Fig. 3.** Comparison of CTDP and TDLP across different bounding-box features (X, Y, W, H, C) measured by HOTA on SportsMOT validation set.

TDLP consistently outperforms CTDP across all feature subsets, with the gap widening as more features are introduced. This highlights a fundamental difference between the objectives: contrastive learning enforces a global embedding structure in which all features must align within a shared metric space, whereas link prediction learns a local similarity function that can selectively weight informative components. As a result, TDLP benefits from richer feature combinations, while CTDP becomes increasingly constrained as heterogeneous features are added.

To further analyze why TDLP outperforms CTDP in the single-feature setting (Figure 3), we design a controlled experiment that isolates association behavior. A single track is observed over a short history and matched to one positive detection (its true continuation) and several systematically varied negative detections. We evaluate two failure modes during linear assignment: (i) a *rank test*, which checks whether the positive detection is ranked above all negatives, and (ii) a *threshold test*, which verifies whether negatives remain below the association threshold when the positive detection is absent. Failing the rank test guarantees an ID switch, as a negative detection is preferred over the true continuation. Failing the threshold test leads to an ID switch when the true detection is missed, since negatives are not rejected by the gating mechanism during linear assignment.

Figure 4 highlights a clear contrast between CTDP and TDLP. Both methods perform well in rank tests, indicating similar behavior when detector recall is high. However, only TDLP remains reliable in threshold tests: CTDP fails to reject negative detections across all configurations, revealing strong sensitivity to detector false negatives. In contrast, TDLP consistently suppresses negatives,

motion pattern		$n_0$	$n_1$	$n_2$	$n_3$
static	.	.	.	.	.
static conf decay	.	.	.	.	.
linear	.	.	.	.	.
linear conf decay	.	.	.	.	.
nonlinear accel	.	.	.	.	.
nonlinear curve	.	X	.	X	.

motion pattern		$n_0$	$n_1$	$n_2$	$n_3$
static	.	.	.	.	.
static conf decay	.	.	.	.	.
linear	.	.	.	.	.
linear conf decay	.	.	.	.	.
nonlinear accel	.	.	.	.	.
nonlinear curve	.	.	.	.	.

motion pattern		$n_0$	$n_1$	$n_2$	$n_3$
static	X	X	X	X	.
static conf decay	X	X	X	X	.
linear	X	X	X	X	.
linear conf decay	X	X	X	X	.
nonlinear accel	X	X	X	X	.
nonlinear curve	X	X	X	X	.

motion pattern		$n_0$	$n_1$	$n_2$	$n_3$
static	.	.	.	.	.
static conf decay	.	.	.	.	.
linear	.	.	.	.	.
linear conf decay	.	.	.	.	.
nonlinear accel	.	.	.	.	.
nonlinear curve	.	.	.	.	X

**Fig. 4.** Pass/fail matrices for CTDP and TDLP. Dots indicate correct outcomes; shaded cells (X) mark failures leading to ID switches. See Appendix B.

demonstrating robustness in scenarios where linear assignment most often fails. This difference arises from the contrastive objective of CTDP, which maps spatially nearby boxes to similar embeddings, whereas TDLP maintains sharper discriminative boundaries. Full experimental details are provided in Appendix B.

## 5 Conclusion

We propose Track–Detection Link Prediction (TDLP), a learning-based data association framework that formulates multi-object tracking as per-frame link prediction between tracks and detections. TDLP learns association directly from data, avoids handcrafted heuristics, and remains computationally more efficient than fully end-to-end trackers while preserving the modularity of tracking-by-detection pipelines. Extensive experiments on multiple challenging benchmarks show that TDLP outperforms state-of-the-art heuristic-based and end-to-end approaches, particularly in scenarios with non-linear motion. Even when using only bounding-box features, TDLP achieves strong performance, highlighting the effectiveness of link prediction for geometric association. Through controlled analysis, we expose the limitations of metric-learning–based association. TDLP’s main limitation is computational cost, which arises from quadratic track–detection scoring and transformer-based encoders. Future work will explore longer temporal windows and architectural optimizations to reduce this cost.

## A Implementation details

**Architecture.** Figure 2 illustrates the TDLP architecture. For bounding boxes and pose keypoints, both static and motion encoders are implemented as MLPs with two linear layers, LayerNorm [5], SiLU [18], and dropout [37]. Appearance features use only a static encoder following CAMELTrack [36]. All feature embeddings are 512-dimensional and are processed by modality-specific transformer

temporal encoders [43] with 4 layers and 8 heads. The resulting features are projected to 1024 dimensions, summed into a multi-modal representation, and passed through an object interaction encoder with the same architecture. The link prediction head is a two-layer MLP with LayerNorm and SiLU.

**Training.** For each feature modality, TDLP is pretrained using AdamW [33,27] with a cosine annealing scheduler [26], 2 warmup epochs, learning rate  $5 \times 10^{-2}$ , weight decay  $1 \times 10^{-2}$ , and gradient clipping at 1.0. The multi-modal model is then fine-tuned for 10 epochs with 1 warmup epoch, learning rate  $1 \times 10^{-5}$ , and weight decay  $1 \times 10^{-3}$ . The BCE positive class weight is set to 10. Clip length is 50 for DanceTrack, MOTChallenge, and BEE24, and 150 for SportsMOT and SoccerNet to support long-term occlusions, making TDLP the first online tracker to handle this setting.

**Object detection and feature extraction models.** We use the official YOLOX detector for DanceTrack [21], the dataset-provided YOLOX for SportsMOT and SoccerNet [16], TOPICTrack’s detector for BEE24 [12], and ByteTrack’s YOLOX for all MOTChallenge benchmarks. To ensure a transparent comparison, TDLP uses the same pose keypoints and appearance features as CAMELTrack [36], differing only in the association mechanism.

**Tracker hyper-parameters.** Definitions are provided in Section 3.3. Values are listed in the order: DanceTrack, SportsMOT, BEE24, and MOTChallenge, with SoccerNet matching SportsMOT. The detection threshold  $\theta_{\text{det}}$  is 0.4, 0.1, 0.6, and 0.5; the link threshold  $\theta_{\text{link}}$  is 0.015, 0.01, 0.65, and 0.05; the initialization time  $T_{\text{init}}$  is 3, 1, 0, and 1; the initialization confidence  $\theta_{\text{new}}$  is 0.9, 0.4, 0.6, and 0.55; and the maximum lost duration  $T_{\text{lost}}$  is 50, 150, 50, and 50 frames.

## B Additional results

**Additional benchmarks.** The MOTChallenge [17] benchmark consists of short video sequences with mostly linear pedestrian motion and limited appearance variation, and lacks an official validation split.. We report results on MOT17 in Table 6. On this dataset, our model underperforms compared to heuristic-based methods, primarily due to the limited amount of training data and the absence of a validation split, which prevents proper hyper-parameter tuning. Heuristic-based trackers commonly split sequences into two halves [47,4,11,29,3,2] to mitigate these issues; however, this strategy is suboptimal in our case, as the model could overfit to appearance cues in later segments of the sequence. Metric-learning-based approaches rely on inter-clip sampling, which partially alleviates these limitations, as reflected in Table 6, where CAMELTrack outperforms our method by 1.8% in terms of HOTA. We leave a more thorough investigation of these limitations to future work.

For SoccerNet [15], the dataset comprises video clips of soccer matches with the goal of tracking players, making it closely related to SportsMOT in terms of domain and visual characteristics. The results are reported in Table 7. TDLP achieves the best overall performance across all metrics, while TDLP-bbox consistently outperforms all methods that rely solely on detector bounding box

Method	HOTA	DetA	AssA	MOTA	IDF1
<i>e2e</i>					
MOTR [46]	57.8	60.3	55.7	73.4	68.6
MeMOTR [19]	58.8	59.6	58.4	72.8	71.5
MOTIP [20]	59.2	62.0	56.9	75.5	71.2
<i>tbd</i>					
FairMOT [48]	59.3	—	—	73.7	72.3
OC-SORT [11]	61.7	—	—	76.0	76.2
ByteTrack [47]	<b>62.8</b>	—	—	<b>78.7</b>	<b>77.1</b>
GHOST [35]	<b>62.8</b>	—	—	<b>78.7</b>	<b>77.1</b>
CAMELTrack [36]	62.4	63.6	<b>61.4</b>	78.5	76.5
<b>TDLP (ours)</b>	60.6	63.4	58.2	78.0	73.7

**Table 6:** Evaluation results on the MOT17 test set.

Method	HOTA	DetA	AssA	MOTA	IDF1
<i>tbd (bbox features)</i>					
SORT [6]	48.3	<b>58.9</b>	39.7	<b>68.6</b>	53.4
ByteTrack [47]	50.3	<b>58.9</b>	43.1	<b>68.8</b>	57.2
<b>TDLP-bbox (ours)</b>	52.2	58.5	46.7	67.7	63.6
<i>tbd (extra features)</i>					
CAMELTrack [36]	54.2	58.7	50.3	67.4	67.5
<b>TDLP (ours)</b>	<b>56.3</b>	58.7	<b>54.2</b>	67.4	<b>70.4</b>

**Table 7:** Evaluation results on the SoccerNet test set.

features. In particular, TDLP-bbox improves HOTA by 1.9% over the strongest bbox-only baseline and TDLP outperforms CAMELTrack by 2.1%.

**Computational efficiency.** We evaluate the computational efficiency of TDLP-bbox and TDLP on DanceTrack and SportsMOT using a consumer-grade GPU (Table 8), and report CAMELTrack under the same setup for reference, which is up to twice as fast as end-to-end methods [36,46]. TDLP’s link prediction scales quadratically with the number of objects, whereas CAMELTrack scales linearly; as a result, TDLP-bbox achieves substantially faster association on moderately crowded scenes but incurs higher costs in extreme crowding, with a similar trend observed for TDLP on SportsMOT.

Method	DanceTrack					SportsMOT				
	Det	KP	App	Assoc	E2E	Det	KP	App	Assoc	E2E
TDLP-bbox (ours)	9.9	—	—	<b>96.2</b>	<b>9.0</b>	9.1	—	—	<b>41.7</b>	<b>7.5</b>
TDLP (ours)	9.9	12.5	43.1	31.5	4.2	9.1	3.6	39.3	10.8	2.0
CAMELTrack [36]	9.9	12.5	43.1	32.2	4.3	9.1	3.6	39.3	20.1	2.2

**Table 8:** Computational efficiency comparison in terms of FPS (Frames Per Second). *Det*, *KP*, and *App* denote detection, keypoint, and appearance extraction, while *Assoc* and *E2E* report association-only and end-to-end inference times.

**CTDP vs. TDLP experiment setting.** We use 50-frame track histories with base box (0.30, 0.20, 0.05, 0.10, 0.95). Negative detections are generated using offsets  $(s, s, s, s, 0)$ ,  $(s, 0, 0, 0, 0)$ ,  $(0, s, 0, 0, 0)$ , and  $(s/2, s/2, 0, 0, -5s)$  with  $s = 0.1$ . Motion patterns include static, static with confidence decay ( $\Delta c = -0.02$ ), linear (0.01, 0.008), linear horizontal drift ( $\Delta x = 0.003$ ,  $\Delta c = -0.01$ ), nonlinear acceleration ( $a_x = 0.0001$ ,  $a_y = 0.00005$ ), and curved motion ( $\Delta x = 0.002$ ,  $a_y = -0.0003$ ).

## References

1. Adžemović, M.: Deep learning-based multi-object tracking: A comprehensive survey from foundations to state-of-the-art (2025), <https://arxiv.org/abs/2506.13457>
2. Adžemović, M., Tadić, P., Petrović, A., Nikolić, M.: Engineering an efficient object tracker for non-linear motion. arXiv preprint arXiv:2407.00738 (2024), <https://arxiv.org/abs/2407.00738>
3. Adžemović, M., Tadić, P., Petrović, A., Nikolić, M.: Beyond kalman filters: deep learning-based filters for improved object tracking. Machine Vision and Applications **36**(1), 20 (2024). <https://doi.org/10.1007/s00138-024-01644-x>, <https://doi.org/10.1007/s00138-024-01644-x>
4. Aharon, N., Orfaig, R., Bobrovsky, B.Z.: Bot-sort: Robust associations multi-pedestrian tracking. In: arXiv preprint (2022), arxiv: 2206.14651
5. Ba, J.L., Kiros, J.R., Hinton, G.E.: Layer normalization. In: arXiv preprint (2016), arxiv: 1607.06450
6. Bewley, A., Ge, Z., Ott, L., Ramos, F., Upcroft, B.: Simple online and realtime tracking. In: 2016 IEEE International Conference on Image Processing (ICIP). pp. 3464–3468 (2016). <https://doi.org/10.1109/ICIP.2016.7533003>
7. Bozek, K., Hebert, L., Mikheyev, A., Stephens, G.: Towards dense object tracking in a 2d honeybee hive. pp. 4185–4193 (06 2018). <https://doi.org/10.1109/CVPR.2018.00440>
8. Brasó, G., Leal-Taixé, L.: Learning a neural solver for multiple object tracking. In: The IEEE Conference on Computer Vision and Pattern Recognition (CVPR) (June 2020)
9. Caesar, H., Bankiti, V., Lang, A.H., Vora, S., Liong, V.E., Xu, Q., Krishnan, A., Pan, Y., Baldan, G., Beijbom, O.: muscenes: A multimodal dataset for autonomous driving. arXiv preprint arXiv:1903.11027 (2019)
10. Cai, J., Xu, M., Li, W., Xiong, Y., Xia, W., Tu, Z., Soatto, S.: Memot: Multi-object tracking with memory. In: 2022 IEEE/CVF Conference on Computer Vision and Pattern Recognition (CVPR). pp. 8080–8090 (2022). <https://doi.org/10.1109/CVPR52688.2022.00792>
11. Cao, J., Pang, J., Weng, X., Khirodkar, R., Kitani, K.: Observation-centric sort: Rethinking sort for robust multi-object tracking. In: 2023 IEEE/CVF Conference on Computer Vision and Pattern Recognition (CVPR). pp. 9686–9696 (2023). <https://doi.org/10.1109/CVPR52729.2023.00934>
12. Cao, X., Zheng, Y., Yao, Y., Qin, H., Cao, X., Guo, S.: Topic: A parallel association paradigm for multi-object tracking under complex motions and diverse scenes. IEEE Transactions on Image Processing **34**, 743–758 (2025). <https://doi.org/10.1109/TIP.2025.3526066>
13. Cetintas, O., Brasó, G., Leal-Taixé, L.: Unifying short and long-term tracking with graph hierarchies. In: Proceedings of the IEEE/CVF Conference on Computer Vision and Pattern Recognition (CVPR). pp. 22877–22887 (June 2023)
14. Chen, B., Li, P., Bai, L., Qiao, L., Shen, Q., Li, B., Gan, W., Wu, W., Ouyang, W.: Backbone is all your need: A simplified architecture for visual object tracking. arXiv preprint arXiv:2203.05328 (2022)
15. Cioppa, A., Giancola, S., Deliege, A., Kang, L., Zhou, X., Cheng, Z., Ghanem, B., Van Droogenbroeck, M.: Soccernet-tracking: Multiple object tracking dataset and benchmark in soccer videos. In: Proceedings of the IEEE/CVF Conference on Computer Vision and Pattern Recognition. pp. 3491–3502 (2022)

16. Cui, Y., Zeng, C., Zhao, X., Yang, Y., Wu, G., Wang, L.: Sportsmot: A large multi-object tracking dataset in multiple sports scenes. In: 2023 IEEE/CVF International Conference on Computer Vision (ICCV). pp. 9887–9897 (2023). <https://doi.org/10.1109/ICCV51070.2023.00910>
17. Dendorfer, P., Ošep, A., Milan, A., Schindler, K., Cremers, D., Reid, I., Roth, S., Leal-Taixé, L.: Motchallenge: A benchmark for single-camera multiple target tracking. International Journal of Computer Vision **129**(4), 845–881 (2021). <https://doi.org/10.1007/s11263-020-01393-0>, <https://doi.org/10.1007/s11263-020-01393-0>
18. Elfwing, S., Uchibe, E., Doya, K.: Sigmoid-weighted linear units for neural network function approximation in reinforcement learning. Neural Networks **107**, 3–11 (2018). <https://doi.org/https://doi.org/10.1016/j.neunet.2017.12.012>, special issue on deep reinforcement learning
19. Gao, R., Wang, L.: Memotr: Long-term memory-augmented transformer for multi-object tracking. In: 2023 IEEE/CVF International Conference on Computer Vision (ICCV). pp. 9867–9876 (2023). <https://doi.org/10.1109/ICCV51070.2023.00908>
20. Gao, R., Zhang, Y., Wang, L.: Multiple object tracking as id prediction (2024), <https://arxiv.org/abs/2403.16848>
21. Ge, Z., Liu, S., Wang, F., Li, Z., Sun, J.: Yolox: Exceeding yolo series in 2021 (2021), <https://arxiv.org/abs/2107.08430>
22. Han, X., Oishi, N., Tian, Y., Ucurum, E., Young, R., Chatwin, C., Birch, P.: Etrack: enhanced temporal motion predictor for multi-object tracking. Applied Intelligence **55**(1), 33 (2024). <https://doi.org/10.1007/s10489-024-05866-4>, <https://doi.org/10.1007/s10489-024-05866-4>
23. Hossam, A., Ramadan, A., Magdy, M., Abdelwahab, R., Ashraf, S., Mohamed, Z.: Revolutionizing retail analytics: Advancing inventory and customer insight with ai. In: 2024 International Conference on Machine Intelligence and Smart Innovation (ICMISI). pp. 64–69 (2024). <https://doi.org/10.1109/ICMISI61517.2024.10580424>
24. Huang, H.W., Yang, C.Y., Sun, J., Kim, P.K., Kim, K.J., Lee, K., Huang, C.I., Hwang, J.N.: Iterative Scale-Up ExpansionIoU and Deep Features Association for Multi-Object Tracking in Sports . In: 2024 IEEE/CVF Winter Conference on Applications of Computer Vision Workshops (WACVW). pp. 163–172 (2024). <https://doi.org/10.1109/WACVW60836.2024.00024>
25. Liu, Z., Wang, X., Wang, C., Liu, W., Bai, X.: Sparsetrack: Multi-object tracking by performing scene decomposition based on pseudo-depth (2025). <https://doi.org/10.1109/TCSVT.2024.3524670>
26. Loshchilov, I., Hutter, F.: Sgdr: Stochastic gradient descent with warm restarts. arXiv preprint arXiv:1608.03983 (2017)
27. Loshchilov, I., Hutter, F.: Decoupled weight decay regularization. In: 7th International Conference on Learning Representations (ICLR) (2019)
28. Luiten, J., Ošep, A., Dendorfer, P., Torr, P., Geiger, A., Leal-Taixé, L., Leibe, B.: Hota: A higher order metric for evaluating multi-object tracking. International Journal of Computer Vision **129**(2), 548–578 (2021). <https://doi.org/10.1007/s11263-020-01375-2>
29. Maggiolino, G., Ahmad, A., Cao, J., Kitani, K.: Deep oc-sort: Multi-pedestrian tracking by adaptive re-identification. In: 2023 IEEE International Conference on Image Processing (ICIP). pp. 3025–3029 (2023). <https://doi.org/10.1109/ICIP49359.2023.10222576>

30. Meinhardt, T., Kirillov, A., Leal-Taixé, L., Feichtenhofer, C.: Trackformer: Multi-object tracking with transformers. In: 2022 IEEE/CVF Conference on Computer Vision and Pattern Recognition (CVPR). pp. 8834–8844 (2022). <https://doi.org/10.1109/CVPR52688.2022.00864>
31. Miah, M., Bilodeau, G.A., Saunier, N.: Learning data association for multi-object tracking using only coordinates. *Pattern Recognition* **160**, 111169 (2025). <https://doi.org/https://doi.org/10.1016/j.patcog.2024.111169>, <https://www.sciencedirect.com/science/article/pii/S0031320324009208>
32. Oord, A.v.d., Li, Y., Vinyals, O.: Representation learning with contrastive predictive coding. *arXiv preprint arXiv:1807.03748* (2018)
33. P, D., Kingma, Ba, J.: Adam: A method for stochastic optimization. In: 3rd International Conference on Learning Representations (ICLR) (2015)
34. Ramshaw, L., E, R., Tarjan: On minimum-cost assignments in unbalanced bipartite graphs. In: HP Laboratories (2012)
35. Seidenschwarz, J., Brasó, G., Serrano, V.C., Elezi, I., Leal-Taixé, L.: Simple cues lead to a strong multi-object tracker. In: 2023 IEEE/CVF Conference on Computer Vision and Pattern Recognition (CVPR). pp. 13813–13823 (2023). <https://doi.org/10.1109/CVPR52729.2023.01327>
36. Somers, V., Standaert, B., Joos, V., Alahi, A., Vleeschouwer, C.D.: Cameltrack: Context-aware multi-cue exploitation for online multi-object tracking (2025), <https://arxiv.org/abs/2505.01257>
37. Srivastava, N., Hinton, G., Krizhevsky, A., Sutskever, I., Salakhutdinov, R.: Dropout: A simple way to prevent neural networks from overfitting. *Journal of Machine Learning Research* **15**(56), 1929–1958 (2014)
38. Stanojevic, V.D., Todorovic, B.T.: Boosttrack: boosting the similarity measure and detection confidence for improved multiple object tracking. *Machine Vision and Applications* **35**(3), 53 (April 2024). <https://doi.org/10.1007/s00138-024-01531-5>, <https://doi.org/10.1007/s00138-024-01531-5>
39. Sun, P., Cao, J., Jiang, Y., Yuan, Z., Bai, S., Kitani, K., Luo, P.: Dancetrack: Multi-object tracking in uniform appearance and diverse motion. In: 2022 IEEE/CVF Conference on Computer Vision and Pattern Recognition (CVPR). pp. 20961–20970 (2022). <https://doi.org/10.1109/CVPR52688.2022.02032>
40. Urbann, O., Bredtmann, O., Otten, M., Richter, J.P., Bauer, T., Zibriczky, D.: Online and real-time tracking in a surveillance scenario. In: 5th Workshop on Long-term Human Motion Prediction (2021), arxiv: 2106.01153
41. Wojke, N., Bewley, A., Paulus, D.: Simple online and realtime tracking with a deep association metric. In: 2017 IEEE International Conference on Image Processing (ICIP). pp. 3645–3649 (2017). <https://doi.org/10.1109/ICIP.2017.8296962>
42. Xiao, C., Cao, Q., Zhong, Y., Lan, L., Zhang, X., Luo, Z., Tao, D.: Motiotiontrack: Learning motion predictor for multiple object tracking. *Neural Networks* **179**, 106539 (2024). <https://doi.org/https://doi.org/10.1016/j.neunet.2024.106539>
43. Xu, Z., Zhan, X., Xiu, Y., Suzuki, C., Shimada, K.: Onboard dynamic-object detection and tracking for autonomous robot navigation with rgb-d camera. *IEEE Robotics and Automation Letters* **9**(1), 651–658 (2024). <https://doi.org/10.1109/LRA.2023.3334683>
44. Yang, M., Han, G., Yan, B., Zhang, W., Qi, J., Lu, H., Wang, D.: Hybrid-sort: Weak cues matter for online multi-object tracking. In: Proceedings of the AAAI Conference on Artificial Intelligence. vol. 38, pp. 6504–6512 (2024). <https://doi.org/10.1609/aaai.v38i7.28471>

45. Yi, K., Luo, K., Luo, X., Huang, J., Wu, H., Hu, R., Hao, W.: Ucmctrack: Multi-object tracking with uniform camera motion compensation. *Proceedings of the AAAI Conference on Artificial Intelligence* **38**(7), 6702–6710 (Mar 2024). <https://doi.org/10.1609/aaai.v38i7.28493>
46. Zeng, F., Dong, B., Zhang, Y., Wang, T., Zhang, X., Wei, Y.: Motr: End-to-end multiple-object tracking with transformer. In: *European Conference on Computer Vision (ECCV)* (2022)
47. Zhang, Y., Sun, P., Jiang, Y., Yu, D., Weng, F., Yuan, Z., Luo, P., Liu, W., Wang, X.: Bytetrack: Multi-object tracking by associating every detection box. In: Avidan, S., Brostow, G., Cissé, M., Farinella, G.M., Hassner, T. (eds.) *Computer Vision – ECCV 2022*. pp. 1–21. Springer Nature Switzerland, Cham (2022). [https://doi.org/10.1007/978-3-031-20047-2\\_1](https://doi.org/10.1007/978-3-031-20047-2_1)
48. Zhang, Y., Wang, C., Wang, X., Zeng, W., Liu, W.: Fairmot: On the fairness of detection and re-identification in multiple object tracking. *International Journal of Computer Vision* **129**(11), 3069–3087 (Sep 2021). <https://doi.org/10.1007/s11263-021-01513-4>